# Waterworlds May Have Better Climate Buffering Capacities than Their Continental Counterparts

Benjamin P. C. Hayworth[1] and Bradford J. Foley[1,2]

[1] Pennsylvania State University Department of Geosciences, USA; bph8@psu.edu
[2] Pennsylvania State University Center for Exoplanets and Habitable Worlds, USA

## Abstract

The long-term habitability of a planet is often assumed to be controlled by its ability to cycle carbon between the solid planetary interior and atmosphere. This process allows the planet to respond to external forcings (i.e., changes in insolation, changes in volcanic outgassing rates, etc.) and regulate its surface temperature through negative feedbacks on atmospheric $CO_2$ involved in silicate weathering. Continental weathering and seafloor weathering rates have different, non-linear dependencies on $pCO_2$ and will respond differently to changes in external forcings. Because waterworlds (planets with only seafloor weathering) have a weaker $pCO_2$ dependence than continental worlds (such as modern Earth), we find that waterworlds are better at resisting changes in surface temperature resulting from perturbations in insolation than their continental counterparts, and may be more habitable in this respect.

*Unified Astronomy Thesaurus concepts:* Habitable planets (695); Exoplanets (498); Extrasolar rocky planets (511); Ocean planets (1151); Carbon dioxide (196)

## 1. Introduction

The canonical habitable zone (HZ) is defined as the orbital separations between which a terrestrial planet can have surface liquid water (Kasting et al. 1993). The underlying assumption to the width of the traditional habitable zone is that terrestrial planets will have an active carbonate-silicate cycle that stabilizes their climate against changes in stellar irradiation by regulating atmospheric $CO_2$ (Walker et al. 1981; Kasting et al. 1993; Berner & Berner 2004; Catling et al. 2019). This allows for temperate climates to exist at a range of orbital separations between the outer and inner edges of the HZ.

Most modern modeling of silicate weathering uses some form of the parameterization based upon Walker et al. (1981) for continental weathering that includes both a temperature and direct $pCO_2$ dependence (Berner & Kothavala 2001; Menou 2015; Kadoya & Tajika 2019; Krissansen-Totton & Catling 2017). More recent work has attempted to differentiate between the weathering on continents versus the weathering on the seafloor. However, the dependence of seafloor weathering on surface temperature and the partial pressure of $CO_2$ are likely different than for continental weathering. Previous studies of seafloor weathering typically assumed that it depended only weakly on $pCO_2$, and had no temperature dependence (Sleep & Zahnle 2001; Abbot et al. 2012). As a result, Abbot et al. (2012) and Foley (2015) concluded that exposed land may be necessary for climate buffering via the carbonate-silicate cycle, albeit only small land fractions of $\sim$1% were needed due to the strong feedback provided by continental weathering, and assumed weak seafloor weathering feedback. However, recent observational work by Coogan & Dosso (2015) and Coogan & Gillis (2013) shows that a strong temperature dependence on seafloor weathering may exist. Additional work to parameterize this new seafloor weathering dependence (Krissansen-Totton & Catling 2017; Krissansen-Totton et al. 2018) shows that the seafloor weathering rate depends differently on surface temperature and $pCO_2$ than continental weathering—thus waterworlds or

terrestrial planets with varying ocean coverages will have differing climate responses to external forcing.

Abbot et al. (2012) compared the climate buffering capacity of waterworlds and continental planets (like the Earth). They found that waterworlds had poor climate buffering capacities (CBCs), or ability to resist changes in surface temperature in response to external forcings, compared to planets with continental land fractions above 0.01. The inability of waterworld planets to buffer their climates was largely a result of assuming that seafloor weathering lacked a direct temperature dependence, and only depended directly on atmospheric $CO_2$ (Abbot et al. 2012; Sleep & Zahnle 2001). In this work, we use the updated seafloor weathering parameterization from Krissansen-Totton & Catling (2017), which includes a strong temperature dependence, to re-explore the question of ocean coverage and climate buffering capacity. We find that due to seafloor weathering's weak $pCO_2$ dependence and strong temperature dependence, planets dominated by seafloor weathering are better able to buffer their climate against changes in luminosity. A strong temperature dependence and weak direct $pCO_2$ dependence results in strong climate buffering, because in this situation changes in $CO_2$ alone have little effect on the weathering rate. The only way to bring weathering and degassing into balance after a change in luminosity is for surface temperature to recover to near its previous level (Sleep & Zahnle 2001; Pierrehumbert 2010; Abbot 2016). We use simple weathering and climate models to ascertain how the carbonate-silicate cycle on planets with different ocean coverage responds to changes in insolation and volcanic outgassing rates. We argue that waterworlds (or worlds where silicate weathering is dominated by seafloor weathering) will have better climate buffering capacities than Earth-like or continental planets (worlds where silicate weathering is dominated by continental weathering).

For this study, we will exclude waterworlds where the carbonate-silicate cycle is disrupted by either high-pressure ice or suppression of volcanism (Kite & Ford 2018). The habitability of these extreme waterworlds is not controlled by

carbon cycling—and not relevant to this study. Even more recent work by Chambers (2020) shows that when including seafloor weathering, a climate state exists where a planet can be in a stable ice-covered regime, where outgassing is balanced by seafloor weathering. This differs from the conventional school of thought that a planet that is ice covered will cease weathering (as the continents are glaciated) and will accumulate enough $CO_2$ to escape snowball (Abbot 2016; Haqq-Misra et al. 2016). The planet can then repeat this process, and limit cycle between being glaciated and ice-free states. We do not differentiate between climate states that are below 273 K (permanent snowball or limit cycling) in this Letter. This would require us to make assumptions about $CO_2$ exchange between the ocean and atmosphere during snowball states, which is beyond the scope of what is explored here.

In this Letter, we will first lay out the $CO_2$ weathering parameterizations that we use with a simple climate and weathering model (See Section 2.1). We then cover parameter space using this simple model to quantify the impact solar luminosity, ocean coverage, outgassing rate, and parameterization of $pCO_2$ dependence (for both seafloor and continental weathering) have on a planet's ability to buffer changes in surface temperature (See Section 2.2). We verified the results from the simple model against a model where the weathering parameterizations are combined with a 1D radiative-convective climate model to more accurately calculate equilibrium surface temperatures (See Appendix). We fully discuss the implications of our findings in Section 4.

## 2. Weathering Model

We use a weathering model (See Section 2.1) to make initial predictions about how weathering behavior changes as a function of ocean coverage, and other key model parameters. This simple model is first-order accurate based on comparisons to a more sophisticated radiate-convective climate model (see the Appendix).

### 2.1. Theory

To explore general trends in how the surface temperature responds to different outgassing rates and weathering dependencies, we solve for $pCO_2$ given the following formula, assuming a steady state between the weathering flux and outgassing flux:

$$F(pCO_2) = \frac{dpCO_2}{dt} = 0 = V - F_{cw}\frac{1 - f_{oc}}{0.3} - F_{sw}\frac{f_{oc}}{0.7}(8.474), \quad (1)$$

where $f_{oc}$ is the surface fraction of the planet covered by ocean, the factor 8.474 is to convert $Tmol$ of carbon per year to bars of $CO_2$ per gigayear, and $V$ is our volcanic flux of $CO_2$ into the atmosphere-ocean system and is a free parameter. Because both the continental weathering and seafloor weathering terms are tuned to the modern Earth, we normalize them both by dividing by 0.3 and 0.7, respectively, corresponding to the modern-day Earth fractions of land and ocean coverage. $F_{cw}$ is the continental weathering flux given by (Berner 1992;

Menou 2015):

$$F_{cw} = W_{\oplus}\left(\frac{pCO_2}{p_{\oplus}}\right)^{\beta} e^{k_{act}(T_s - T_{\oplus})}(1 + k_{run}[T_s - T_{\oplus}])^{0.65}, \quad (2)$$

where $W_{\oplus}$ and $p_{\oplus}$ are the terrestrial weathering rate and partial pressure of $CO_2$ for modern Earth, respectively. $\beta$ is the $pCO_2$ dependence of the weathering rate and can theoretically range from 0 to 1 (Berner 1992). We use a median value of 0.5 for most of our calculations. $T_{\oplus}$ is the modern Earth's temperature of 288 K. We follow Berner (1994) and use an assumed mineral dissolution activation energy of $k_{act} = 0.09$ $K^{-1}$, and a runoff efficiency factor of $k_{run} = 0.045$ $K^{-1}$. We explore the sensitivity of our results to the choice of activation energy in the Appendix. For all of our calculations, we assume an abiotic planet when fixing our constants. On an inhabited planet such as the Earth, vascular plants set soil pH, weakening the direct $pCO_2$ dependence on continental weathering. A table of all of our parameter values can be found in the Appendix.

We parameterize the seafloor weathering flux, $F_{sw}$, according to Krissansen-Totton & Catling (2017), where it is directly dependent on the ocean water pH and pore-space temperature at the seafloor:

$$F_{sw} = k_{diss}r_{sr}e^{\frac{-E_{bas}}{RT_p}}\left(\frac{[H^+]}{[H^+_{mod}]}\right)^{\gamma}, \quad (3)$$

where $k_{diss}$ is a proportionality constant used to match the modern Earth's seafloor weathering flux, and $r_{sr}$ is the spreading rate. We chose to not vary $r_{sr}$, and instead treat $k_{diss}$ and $r_{sr}$ together as a proportionality constant and use it to tune the model to the results from Krissansen-Totton & Catling (2017). $E_{bas}$ is an activation energy for which we use the median value from Krissansen-Totton & Catling (2017). $\gamma$ is the hydrogen molarity dependence of the weathering rate and can theoretically range from 0 to 0.5 based on a review of basalt dissolution experiments presented in Krissansen-Totton & Catling (2017). They also confirmed this range by inverting their weathering model to statistically constrain values of $\gamma$ given the paleoclimate proxy record available. We use the median value of 0.25 for most of our calculations. $T_p$ is the pore-space temperature, which we linearly relate to surface temperature according to Krissansen-Totton & Catling (2017):

$$T_p = T_s(1.02) - 16.7 \quad (4)$$

Finally, $[H^+]$ is the hydrogen molarity, which is used to estimate the pH dependence of seafloor weathering. To isolate everything in terms of $pCO_2$ we use the relationship derived by Krissansen-Totton et al. (2018):
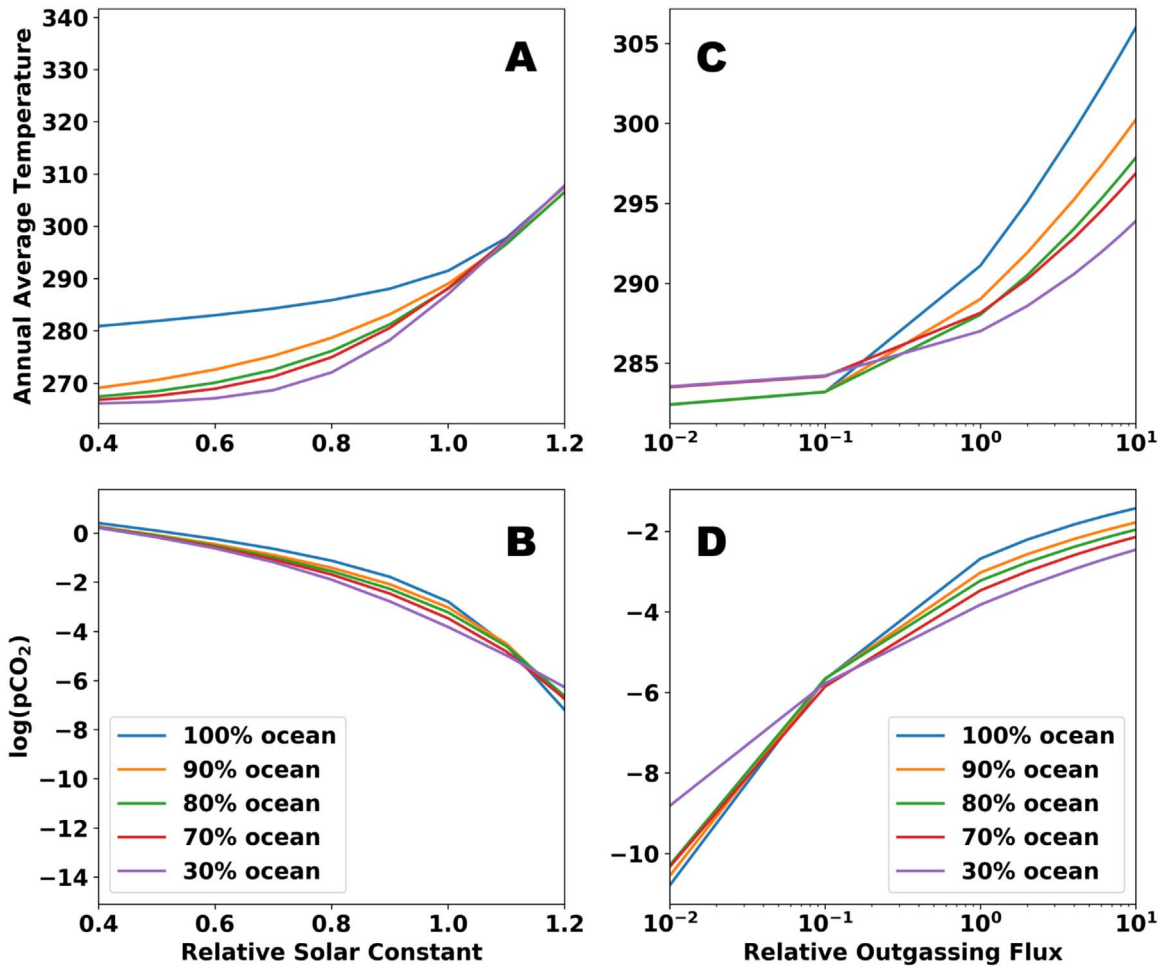
$$[H^+] = 10^{-8.44}pCO_2^{1/1.34}. \quad (5)$$

The last variable that we need to parameterize in terms of $pCO_2$ is surface temperature (see Equations (2) and (4)). We use the following expression from Walker et al. (1981):

$$T_s = 285 + 2(T_e + 254) + 4.6\left(\frac{pCO_2}{3.3 \times 10^{-4}}\right)^{0.346} - 4.6 \quad (6)$$

$$T_e = \left(\frac{S_{eff} * 1370 * [1 - \alpha]}{4\sigma}\right)^{0.25}. \quad (7)$$

By substituting Equations (2)–(7) into Equation (1) we can develop an expression for $pCO_2$ as a function of the relative

**Figure 1.** Panel A shows how surface temperature varies with varied solar luminosity (relative to modern Earth) for different ocean coverages. Panel B shows how $pCO_2$ varies with varied solar luminosity for different ocean coverages. Both Panel A and B assume an Earth-like outgassing rate of $CO_2$. We did not plot solar luminosities greater than 1.2 $S_{eff}$ as the weathering rate dependence on $CO_2$ becomes negligible. Panel C shows how the surface temperature varies with varied $CO_2$ outgassing rates (relative to modern Earth) for different ocean coverages. And Panel D shows how $pCO_2$ varies with varied outgassing rates for different ocean coverages. Panel C and D assume a modern Earth solar constant. All panels assume a fixed planetary albedo of $\alpha = 0.3$.

solar constant, $S_{eff}$, assuming balance between outgassing and weathering. $S_{eff}$ is a scalar multiplicative of the Sun's modern solar luminosity. We use relative solar constant and ocean coverage as free parameters and solve for $pCO_2$ numerically using Newton's Method. As a point of clarification, it may be best to view the percentage of ocean coverage as the fraction of the planet's surface that depends on weathering rates according to Equation (3) rather than Equation (2). While the illustrative example of a waterworld may in fact be correct, a continental world would have many other factors impacting its carbonate-silicate cycle, such as water availability, limited precipitation globally, etc., the effects of which can only be fully explored in a multi-dimensional climate model with hydrologic cycling.

### 2.2. Results

We first assume median values for $\beta$ (see Equation (2)) and $\gamma$ (see Equation (3)) and vary ocean coverage for different relative solar constants (see Equation (7)). In a similar fashion, we also varied the outgassing flux of $CO_2$ (see Equation (1)) while holding the solar flux constant (at an Earth-like value) for varying ocean coverage. The model was tuned to the modern Earth, so all outgassing fluxes are given as fractions of the modern flux.

We can see that for changes in solar luminosity, planets with higher ocean fractions have the smallest change in surface temperature (Figure 1). This trend of having a relatively smaller change in surface temperature to external forcings is what we mean by a planet having better climate buffering. We also see that there is a significant change in climate buffering moving from 90% ocean coverage to 100% ocean coverage. This shift in climate response is due to a transition between continental and seafloor weathering being the dominant sink of $CO_2$. Below, we explore at what ocean fraction this transition from being seafloor weathering dominated to continental weathering dominated takes place. From Figure 1, we can also see that for changes in volcanic outgassing rates, planets with lower ocean fractions have the smallest change in surface temperature. This is due to seafloor weathering's overall weaker temperature plus $pCO_2$ dependence, making waterworlds worse than continental planets at buffering their climate against changes in outgassing. However, as we show later, this weaker buffering to changes in outgassing rate does not significantly impede the development of temperate climates on waterworlds. Additionally, regardless of the ocean coverage, all planets have similar climate buffering capacities at high solar luminosities ($S_{eff} > 1.2$) because $CO_2$ becomes a minor component of the atmosphere and its greenhouse forcing becomes negligible.
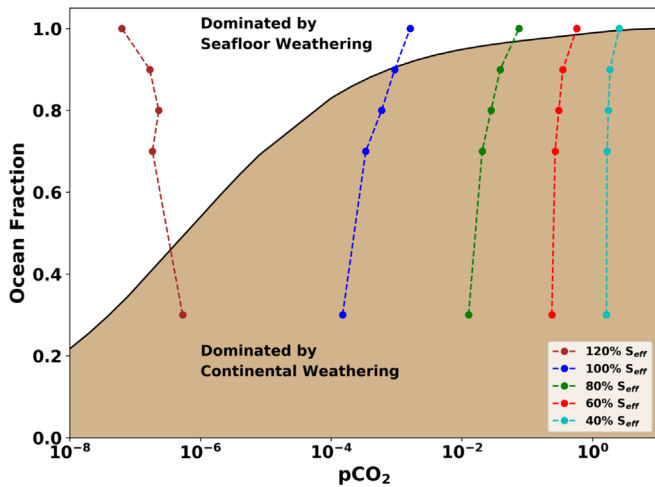
**Figure 2.** The solid curve represents the ocean fraction at which seafloor weathering and continental weathering are equal, as a function of $pCO_2$. We solved this critical ocean fraction curve for different solar luminosities and found that the difference was negligible (the black curve shown is for an $S_{eff}$ of 1.0). If a planet's ocean coverage is above the curve, then seafloor weathering is the dominant sink of $CO_2$, and if a planet's ocean coverage is below the curve, then continental weathering is the dominant sink of $CO_2$. The colored curves and points are data from Figure 1, allowing us to constrain this parameter space by plotting the actual $pCO_2$ values that our model converged toward for a given ocean fraction and solar luminosity. We find that for solar luminosities lower than modern Earth's, an ocean fraction of greater than 90% is needed for seafloor weathering to equal continental weathering.

Based on the results from Figure 1, a planet's buffering capability changes significantly when seafloor weathering becomes the dominant weathering sink, due to the different $pCO_2$ dependencies of seafloor versus continental weathering. We therefore determine the critical ocean fraction where weathering behavior switches from being dominated by seafloor weathering to being dominated by continental weathering by setting $F_{cw} = F_{sw}$, and solving for the ocean fraction:

$$f_{occrit} = \left[(8.474)\left(\frac{0.3}{0.7}\right)\left(\frac{F_{sw}}{F_{cw}}\right) + 1\right]^{-1} \quad (8)$$

We solve for this critical ocean fraction for a range of solar luminosities, setting the rest of the variables equal to the median values that we used for Figure 1, as a function of $pCO_2$ (see Figure 2). The solid curves in Figure 2 correspond to the $f_{occrit}$ at which the weathering fluxes from continental weathering and seafloor weathering are equal. While we calculated $f_{occrit}$ over a range of $pCO_2$ values, only certain $pCO_2$ pressures would be physical for a given solar luminosity using our weathering model. The dashed curves with the points are from our previous results, where we calculated the actual $pCO_2$ of a planet given its solar luminosity and ocean fraction (see Figure 1).

What we find from Figure 2 is that for relative solar luminosities less than or equal to $S_{eff} = 1.0$, the planet requires an ocean fraction between 90% and 99% for the $CO_2$ flux from seafloor weathering to equal the $CO_2$ flux from continental weathering. This is consistent with what we see in Figure 1, and what other authors have found (Abbot et al. 2012; Foley 2015). At lower values of $pCO_2$, i.e., relative solar luminosities higher than modern, a lower ocean fraction is required for seafloor weathering and continental weathering to be equal (for example, $f_{occrit} = \sim40\%$ for $S_{eff} = 1.2$). This is

due to the $pCO_2$ dependence on continental weathering being stronger than for seafloor weathering—allowing the seafloor weathering flux to keep up with the continental weathering flux (which depends strongly on $pCO_2$) at lower ocean fractions.

To better quantify how effective waterworlds versus continental planets are at maintaining their surface temperatures in the face of forcing from solar luminosity or $CO_2$ outgassing, we calculate what we will call the "climate buffering capacity" (CBC) of a planet—which is the change in surface temperature experienced for a given change in solar luminosity, $\frac{dT}{dL}$ (or volcanic outgassing rate $\frac{dT}{dV}$); see Figure 3. A lower value of $\frac{dT}{dL}$ or $\frac{dT}{dV}$ corresponds to a planet having a better CBC (i.e., less change in surface temperature for perturbations in luminosity or outgassing, respectively). The left panel shows that waterworlds in general have a better CBC against changes in luminosity, while continental planets have a better CBC against changes in volcanic outgassing.

For all the calculations up to this point—we have assumed that both $\beta$ and $\gamma$, the continental weathering dependence on $pCO_2$ and the seafloor weathering dependence on pH, respectively, are in the middle of their possible ranges. We next varied both values from their minima to their maxima and calculated the difference in CBC for changing solar luminosity between Earth-like planets (70% ocean) and waterworlds. As the major shift in global weathering being controlled by either continental weathering or seafloor weathering occurs between 90% and 100% ocean coverage (see Figure 2), we chose an Earth-like ocean coverage as representative of land planets. We did the calculation for both Earth's luminosity during the Archean (75% of modern $S_{eff}$) and during the Mid-Proterozoic (88% of modern $S_{eff}$). We chose these solar luminosities to compare to Earth's climate buffering over time, and to avoid unphysical solutions (as we approached higher solar luminosities, such as modern $S_{eff}$, we could no longer solve for unique solutions to equation one using Newton's Method for waterworlds when gamma approached 0).

We find that, in general, waterworlds are better at buffering climate when $\beta$ is $>0.2$, though the exact switch in weathering behavior depends also on the value of $\gamma$. With increasing gamma, the value of beta that delineates the transition from continental weathering to seafloor weathering having the better CBC also increases. The general conclusion from Figure 4 is that waterworlds have better CBCs than their continental counterparts over the majority of parameter space.

As noted previously, while waterworlds are clearly better at buffering climate than continental worlds against changes in luminosity, they are worse at buffering against changes in outgassing rate. In order to explore how this combination of CBCs impacts the overall climate state of the planet, we plot surface temperature as a function of volcanic outgassing rate and solar luminosity, assuming a steady state between weathering and volcanism, as in Kadoya & Tajika (2014).

From Figure 5 it can been seen that as solar luminosity decreases, waterworlds can stay above the freezing point for lower outgassing rates than Earth-like planets; that is, less outgassing is needed to keep the climate temperate at low luminosity on waterworlds. This is due to waterworlds having a better CBC against changes in solar luminosity, and the overall lower weathering rate for seafloor weathering than continental weathering, which allows lower outgassing rates to still promote a temperate climate. The worse CBC against outgassing rate for waterworlds seems to have a minimal effect, as
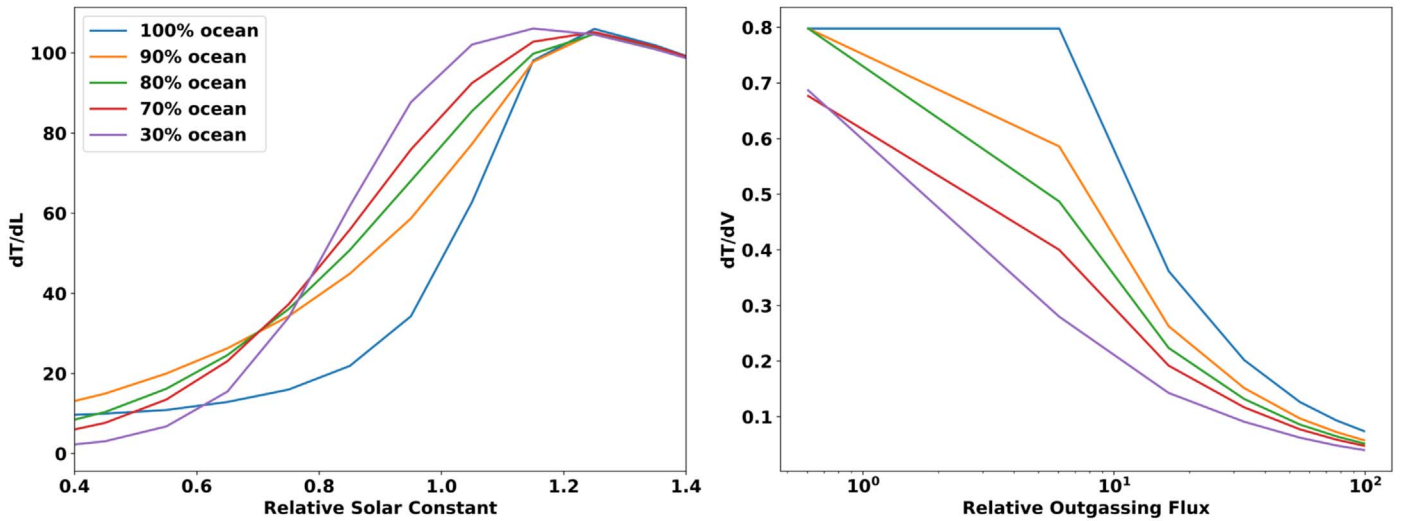
**Figure 3.** CBC of planets with varied ocean coverage. The left panel shows the CBC of planets for changes in solar luminosity, while the right panel shows the CBC of planets for changes in volcanic outgassing. In both cases, a lower value means less change in surface temperature for a given change in solar luminosity or outgassing rate. The units of CBC are in Kelvin per percent change in solar luminosity or volcanic outgassing rate (relative to the modern Earth).
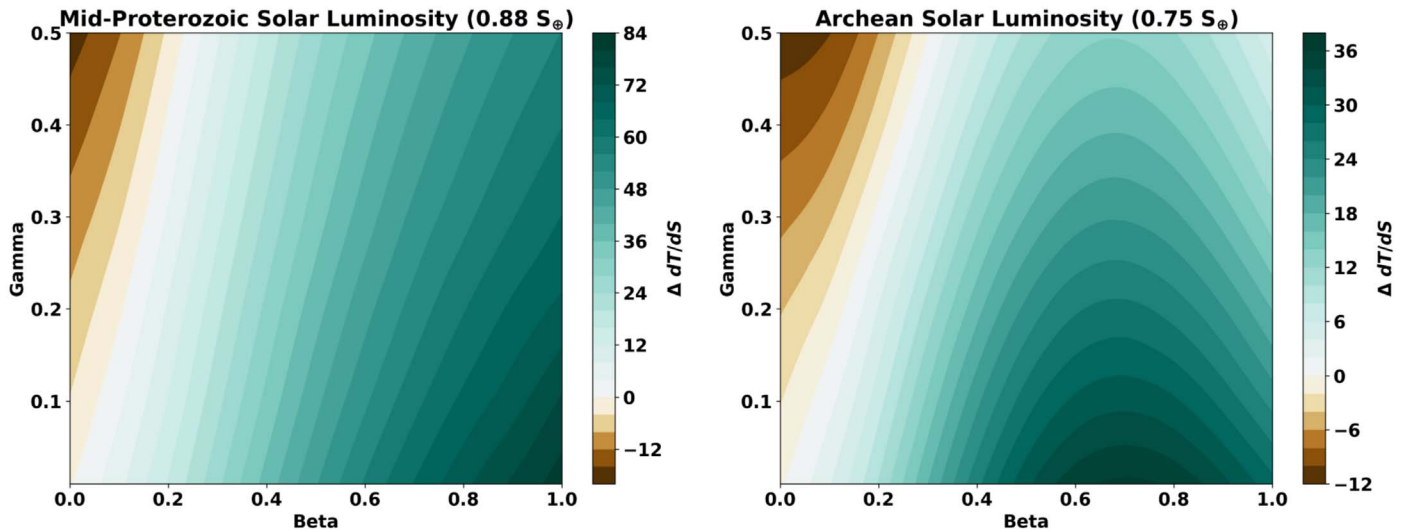


**Figure 4.** Plots of the difference in CBC between an Earth-like planet (70% ocean coverage) and a waterworld. Blue (or positive values) correspond to waterworlds having the better CBC, while brown (negative values) corresponds to Earth-like planets having a better CBC. The left panel is for Mid-Proterozoic solar luminosity (88% $S_{\mathrm{eff}}$) while the right panel is for Archean solar luminosity (75% $S_{\mathrm{eff}}$).
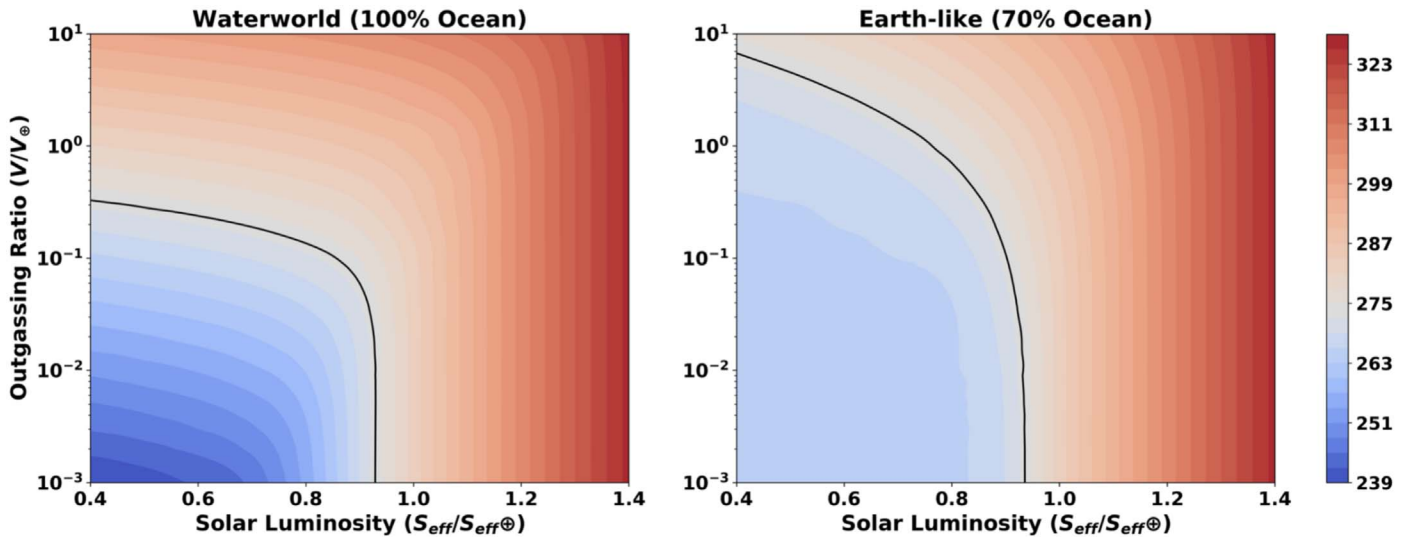
surface temperatures remain above freezing almost independent of volcanic outgassing rates above $\sim 10^{-1}$ present value. It should be noted that for temperatures below 273 K, the planet may be in either a snowball state or limit cycling regime (we cannot differentiate with our model; Haqq-Misra et al. 2016; Abbot 2016). A caveat to this figure is that the simple temperature-$CO_2$ parameterization (see Equation (6)) that we are using does not capture the effect of runaway greenhouse climates. For solar luminosities greater than approximately 1.1 $S_{\mathrm{eff}}$, the climate does not have a stable surface temperature, meaning that the relatively low temperatures in Figure 5 at high luminosities are not physical and the planet would instead enter a runaway greenhouse state.

The results from the weathering model indicate that temperate climates can exist over a wider range of solar luminosities and outgassing rates for waterworlds than for continental planets, due to differences in seafloor weathering versus continental weathering.

## 3. Discussion

These differences in the silicate weathering behavior for varying ocean coverage may impact how these planets evolve climatically. The better climate buffering capacity of waterworlds mean that they will have a smaller temperature distribution throughout the habitable zone than their continental counterparts, and will have more stable climates through time.

As solar luminosity increases on average as a system ages, the planet's volcanic outgassing rates will decrease (Tosi et al. 2017; Dorn et al. 2018; Foley & Smye 2018). The decrease in volcanic outgassing over time would cause the surface temperature of waterworlds to decrease more severely than a continental world under the same conditions. This relationship between planetary thermal evolution, outgassing, and seafloor weathering is explored more explicitly by Höning et al. (2019). Though waterworlds are worse at buffering climate against perturbations in volcanic outgassing than with perturbations in solar luminosity, surface temperatures remain "habitable" over

**Figure 5.** Surface temperature for a given insolation (relative to modern) and volcanic outgassing rate of $CO_2$ (also relative to modern). The red region is for surface temperatures above freezing, while the blue region is for surface temperatures below freezing. The black line corresponds to a surface temperature of 273 K.

3 orders of magnitude of $CO_2$ outgassing rates. Additionally, the surface temperatures for waterworlds are generally higher than that of continental worlds, but not so high that they are more at risk for entering a moist greenhouse regime for the parameter space that we explored (see Figure 5). This is contrasted by continental planets, where surface temperatures fall below freezing for ∼35% changes in solar luminosity. This is why we focus on the CBC against changes in solar luminosity throughout this Letter—as it has a much larger effect, at least as long as planets are outgassing $CO_2$.

Though the overall conclusion is that the average surface temperatures on waterworlds are more resistant to changes in solar luminosity than planets with continents, there are several caveats to what we have explored.

For planets with less ocean coverage, continental weathering rates will be highly dependent on water availability, precipitation patterns, and continental configuration. Modeling of large continents, such as Pangea or the southern highlands on Mars, have shown huge effects on precipitation toward the interior of the continent (Parrish 1993; Donnadieu et al. 2004; Palumbo et al. 2018). This no doubt would affect the weathering behavior for such planets, and is not considered in the above calculations. 3D global climate models would be needed to constrain precipitation patterns, and hence weathering behavior, on such planets. An additional consideration regarding continental coverage is that the Archean earth may have lacked the continental coverage present today, and more closely resembled a waterworld (Flament et al. 2008; Johnson & Wing 2020). An early Earth dominated by seafloor weathering rather than continental weathering may have been better able to remain temperate in the face of a lower solar luminosity.

Orbital configuration will also likely effect global weathering trends for different planets. Tidally locked planets, for example, may only have a limited weathering zone available at the substellar point (Paradise et al. 2019), impacting the effectiveness of continental weathering. However, this may be offset by the persistence of seafloor weathering over much of the planet, as ocean heat transport may keep the pore space temperature high enough for seafloor weathering over a larger fraction of the planet's surface (Hu & Yang 2014). Exploring differences between land-planet and waterworld climate states on tidally

locked planets would require a multi-dimensional weathering and climate model. Tidally locked planets (and slow rotators) will be more sensitive to continental configuration given the warm "eyeball state" where continental weathering is possible (Checlair et al. 2017; Paradise et al. 2019). 3D general circulation models (GCMs) could be needed to explore how sensitive our results in Section 3.2 are to these factors, and how they directly impact the planet's climate buffering potential.

The inverse of our conclusion may be true for young M-dwarf systems, as the solar luminosity increases at a much slower rate on the main-sequence than for a G-type star (Shields et al. 2016). If the outgassing rate for these M-dwarf planets falls off much faster than the rate of solar luminosity increase, then continental worlds may have better CBCs. This would need to be quantified by modeling the outgassing over time for planet's around M-dwarf host stars against the rate of stellar brightening.

Work to analytically constrain both continental and seafloor weathering rates is ongoing (Walker et al. 1981; Berner & Raiswell 1983; Berner & Kothavala 2001; Sleep & Zahnle 2001; Menou 2015; Krissansen-Totton & Catling 2017; Krissansen-Totton et al. 2018). The WHAK weathering formulation (from Walker et al. 1981) that we use (and the authors aforementioned) does not fully capture the complex interactions between tectonics, erosion, and hydrology and their effect on continental weathering, which can be substantial (Kump & Arthur 1997; West et al. 2005; West 2012). The continental weathering formulation from Maher & Chamberlain (2014; MAC) includes more of these physical effects—and Graham & Pierrehumbert (2020) showed that the MAC formulation is much more sensitive to land fraction than our WHAK formulation— meaning we may see a wider variety of climate states for planets with continental fractions greater than 10% (whereas they are very similar in our own model). Assessing the impact of adopting the MAC model in place of the WHAK model on our hypothesis is left as future work. Additionally, all the uncertainties that we have in our parameterizations of continental weathering are also likely to be present in parameterizations of seafloor weathering—all of which is relatively new. Future work to better understand the mechanisms behind seafloor weathering and the best way to model them is needed.

## 4. Conclusion

The different $pCO_2$ dependencies between continental weathering and seafloor weathering causes planets with varying ocean coverage to have different CBCs. Waterworlds have a better CBC than those with continents for changes in solar luminosity. While continental planets have a better CBC than waterworlds for perturbations in volcanic outgassing rate, this is a much smaller effect than that found by varying luminosity.

Our findings are in contrast to those of Abbot et al. (2012), and the reason for this is twofold. First, both their and our parameterizations of seafloor weathering have a weak $pCO_2$ dependence as it is buffered by changes in ocean chemistry, but ours also has a moderately strong temperature dependence (Krissansen-Totton & Catling 2017); this allows seafloor weathering to respond to changes in climate. Second, while continental weathering has a strong temperature dependence, it also has a strong $pCO_2$ dependence. This causes it to "overcompensate" to external forcing, and surface temperature changes more dramatically on planets with land fractions >1% than for waterworlds, with their weaker $pCO_2$ dependence. Our results agree with Abbot et al. (2012) in that a small land fraction can control the climate buffering for a planet, as shown in Figure 2. But our new parameterization of seafloor weathering also provides strong buffering due to its strong temperature dependence.

The purpose of this Letter is to highlight the impact that different $pCO_2$ dependencies on weathering rates have on the climate buffering potential of other worlds. This is an exploratory 0D and 1D study showing the qualitative trends that planets with varying ocean coverage, solar luminosity, and $CO_2$ outgassing flux will possess. Future studies with more sophisticated 3D GCMs are needed to better understand these processes and ascertain whether or not the inclusion of additional physics and free parameters effects the general qualitative trends that we have outlined here.

## Appendix

### A.1. CLIMA + Weathering Model

The results in this Letter use a basic relationship between $pCO_2$ and surface temperature and a fixed planetary albedo. To test if these simplifications impact our results, we coupled our weathering model (Section 2) to a more sophisticated 1D radiative-convective model, CLIMA (Kopparapu et al. 2013; Ramirez & Kaltenegger 2014; Batalha et al. 2016). CLIMA uses a two-stream approximation for radiative transfer and equates total emitted infrared flux to total absorbed solar flux for each
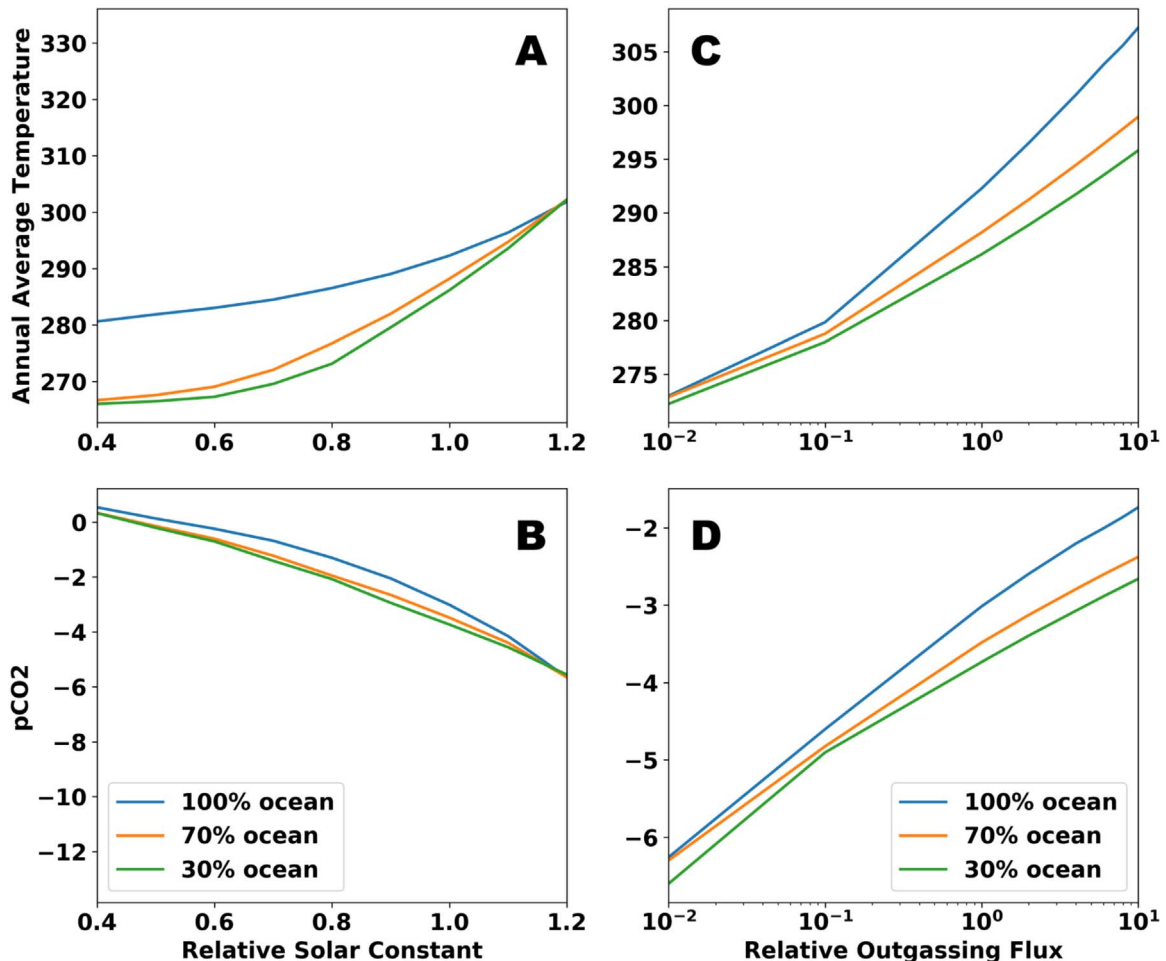


**Figure 6.** Recreation of Figure 1 using the weathering model plus CLIMA.

**Table 1**
List of Parameters Used in the Weathering Model from Section 2, as well as the Values Used Compared to Their Theoretical Ranges from the Literatue

| Parameter | Parameter Definition | Value Used | Values Possible | Source |
|---|---|---|---|---|
| $V$ | Volcanic Outgassing Rate of $CO_2$ | $0.1$–$100 \frac{\text{bars}}{\text{Gyr}}$ | ⋯ | Free Parameter |
| $f_{oc}$ | Ocean Fraction (of Planet's Surface) | $0$–$1$ | ⋯ | Free Parameter |
| $W_\oplus$ | Modern Weathering Rate of $CO_2$ | $7 \frac{\text{bars}}{\text{Gyr}}$ | Tuning Parameter[a] | Menou (2015) |
| $p_\oplus$ | Modern Atmospheric $CO_2$ | $3.3 \times 10^{-4}$ bars | Tuning Parameter[a] | Menou (2015) |
| $\beta$ | pCO$_2$ Dependence of Continental Weathering | $0$–$1$ | $0$–$1$ | Walker et al. (1981) |
| $k_{act}$ | Mineral Dissolution Activation Energy (Continental Weathering) | $0.09$ K$^{-1}$ | $0.06$–$0.135$ K$^{-1}$ | Berner & Kothavala (2001) |
| $k_{run}$ | Runoff Efficiency Factor (Continental Weathering) | $0.045$ K$^{-1}$ | $0.025$–$0.045$ K$^{-1}$ | Berner & Kothavala (2001) |
| $r_{sr} \times k_{diss}$ | ⋯ | $\sim 2.7 \times 10^{15}$ | Tuning Parameter[b] | Krissansen-Totton et al. (2018) |
| $E_{bas}$ | Activation Energy (Seafloor Weathering) | $80 \frac{\text{kJ}}{\text{mol}}$ | $60$–$100 \frac{\text{kJ}}{\text{mol}}$ | Krissansen-Totton et al. (2018) |
| $H^+_{mod}$ | Modern Hydrogen Molarity of Seawater | $10^{-8.2}$ M | Tuning Parameter[a] | Pilson (1998) |
| $\gamma$ | Hydrogen Molarity Dependence of Seafloor Weathering | $0$–$0.5$ | $0$–$0.5$ | Krissansen-Totton & Catling (2017) |
| $S$ | Relative Solar Luminosity | $0.4$–$1.2$ | ⋯ | Free Parameter |
| $\alpha$ | Albedo | $0.3$ | $0$–$1$ | Tuning Parameter[c] |

**Notes.**
[a] Set to tune model to modern Earth.
[b] $r_{sr}$ (spreading rate) is not used as a free parameter, so we tune both $k_{diss}$ and $r_{sr}$ together to match the modern dissolution flux ($\sim 0.45$ Tmol C yr$^{-1}$) for modern Earth conditions, following Krissansen-Totton et al. (2018).
[c] A planetary albedo of 0.3 was used to tune for modern Earth, though this was allowed to vary as a function of pCO$_2$ and $T_s$ in the Appendix.

layer of the stratosphere. Convective lapse rates are solved for with the formulation from Ingersoll (1969) and we assume a moist adiabat with two condensable species (H$_2$O and CO$_2$).

We solve for Equation (1) by first guessing an initial value of pCO$_2$, then running the climate model to convergence. Using the guessed value of pCO$_2$ and the computed surface temperature, we solve Equation (1). If a negative value was returned (too much weathering), we iteratively guess a lower value of pCO2 and repeat. The inverse is true for a positive returned value (too little weathering). We used a convergence criterion of

$$0.99 < \frac{\text{Outgassing}}{\text{Sum of All Weathering Terms}} < 1.01. \qquad (9)$$

The advantage of using a radiative-convective model is twofold. First, the relationship between pCO$_2$ and $T_s$ is highly approximated in Equation (6) and is less accurate for thicker CO$_2$-dominated atmospheres (Kasting & Ackerman 1986). Second, we no longer have to assume a fixed planetary albedo as CLIMA calculates the planetary albedo as a function atmospheric variables.

Using the same weathering model coupled with CLIMA, we redid the calculations for varying solar luminosity, volcanic outgassing, and ocean coverage (Figure 6). There is no change to the qualitative trend found in Section 2.2. This means that 1.) the pCO$_2$–$T_s$ relationship in Equation (6) is consistent with the radiative-convective model results, and 2.) the results are not overly sensitive to changes in planetary albedo. This reaffirms our earlier conclusion that waterworlds buffer better against changes in luminosity but worse against changes in outgassing (though the worse CBC against changes in outgassing rate are not as significant).

### A.2. Sensitivity to Weathering Activation Energies

Another point of uncertainty in our weathering parameterizations is our choice of activation energies ($k_{act}$, $k_{run}$, and $E_{bas}$). In order to compare the activation energies for our continental weathering and seafloor weathering models, we first demonstrate how to relate $k_{act}$, the activation energy for a linear-exponential temperature dependence, as used in Equation (2), to the

corresponding activation energy, $E$, from a full Arrhenius law temperature dependence, as used for seafloor weathering (Equation (3)), as:

$$k_{act} \simeq \frac{E}{RT_\oplus^2} \qquad (10)$$

Here $T_\oplus$ is the modern Earth's temperature of 288 K, and $R$ is the universal gas constant. Then, to use the range of continental weathering activation energies inferred from paleoclimate proxy data by Krissansen-Totton & Catling (2017), we combine the runoff efficiency and mineral dissolution terms, and their separate temperature dependencies controlled by the parameters $k_{act}$ and $k_{run}$, into one linear-exponential term as:

$$e^{k_{act}(T_s - T_\oplus)}(1 + k_{run}[T_s - T_\oplus])^{0.65} \simeq e^{\frac{E_a}{RT_\oplus^2}[T_s - T_\oplus]}. \qquad (11)$$

We then test our new temperature dependence on continental weathering (right-hand side of Equation (11)) against the old (left-hand side of Equation (11)), to make sure that it is consistent with results throughout this Letter. We do this for both the minimum and maximum values of $k_{act}$ and $k_{run}$ (see Table 1) from Berner (1994), and estimate corresponding equivalent values of $E_a$ in order to compare the old and new continental weathering models.

Figure 7 demonstrates that modeling the temperature dependence on continental weathering as a single exponential term is approximately equivalent to the expression used throughout the main text. The advantage of this revised expression is that we now have a single activation energy, $E_a$, that includes of both the runoff and dissolution activation energies together, and is in terms of kJ/mol—making it comparable to the activation energy of seafloor weathering, $E_{bas}$. We then vary the values of $E_a$ and $E_{bas}$ over their prior distributions found in Krissansen-Totton et al. (2018; 14–140 kJ/mol & 60–100 kJ/mol, respectively).

We find from Figure 8 that for the majority of the activation energy parameter space available, waterworlds have better CBCs. It also appears that this depends more strongly on the value of $E_{bas}$ than on the value of $E_a$. Earth-like planets (with
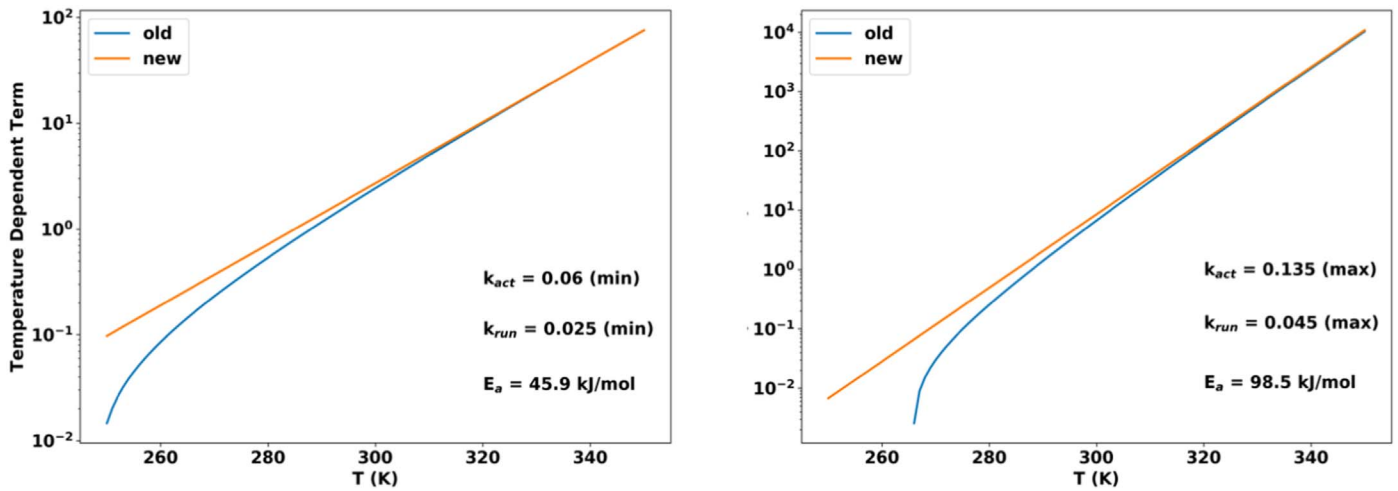
**Figure 7.** Comparison of our old continental weathering temperature dependence vs. our new continental weathering temperature dependence (see Equation (11)) for minimum (left panel) and maximum (right panel) estimates of $k_{\rm act}$ and $k_{\rm run}$, and hence, $E_a$.
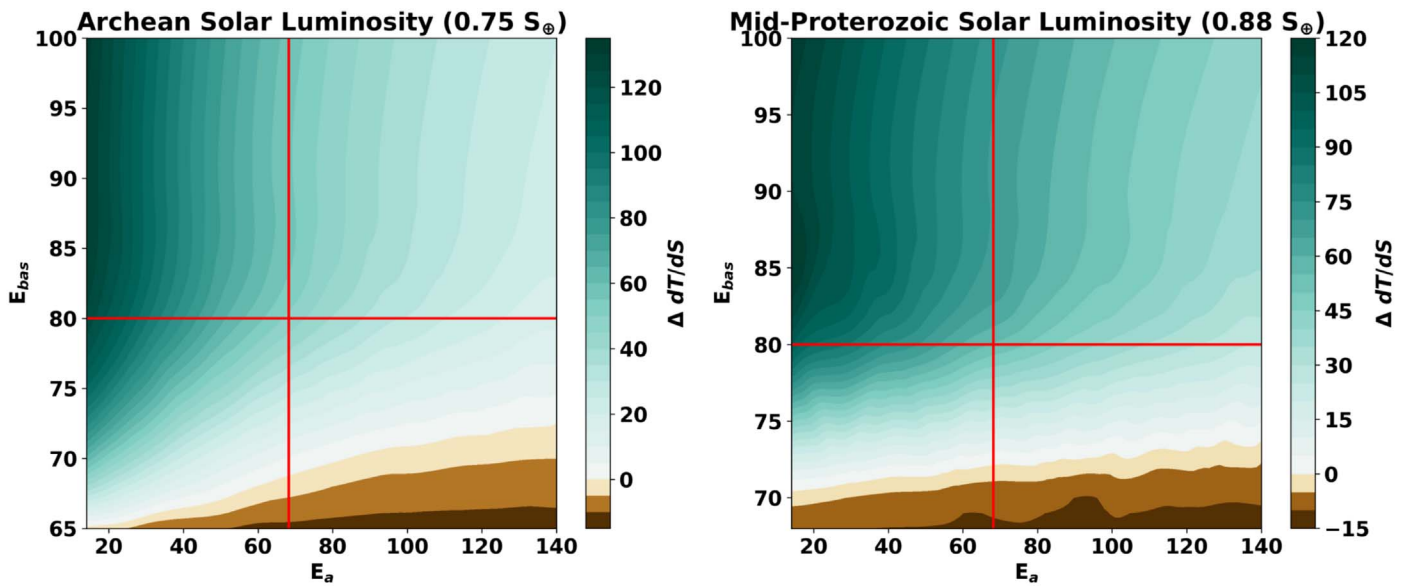


**Figure 8.** Plot showing the sensitivity of CBC on weathering activation energies. $E_a$ is the activation energy for continental weathering, while $E_{bas}$ is the activation energy for seafloor weathering. Gamma and beta are fixed to 0.25 and 0.5, respectively. Positive values of $\Delta dT/dS$ correspond to waterworlds having better CBCs, and negative values of $\Delta dT/dS$ correspond to Earth-like worlds having better CBCs. The red lines correspond to the activation energies used throughout the main text.

70% ocean coverage) may have slightly better CBCs if $E_{\rm bas}$ is low and $E_a$ is high; however, Krissansen-Totton & Catling (2017) argued for a median value of $E_a$ closer to 20 kJ/mol, and a most likely value of $E_{\rm bas} \sim 75$ kJ/mol. This combination of activation energies would reinforce our conclusion that waterworlds have better CBCs than continental worlds.

### ORCID iDs

Bradford J. Foley ⓘ https://orcid.org/0000-0002-6943-3192

### References

Abbot, D. S. 2016, ApJ, 827, 117
Abbot, D. S., Cowan, N. B., & Ciesla, F. J. 2012, ApJ, 756, 178
Batalha, N. E., Kopparapu, R. K., Haqq-Misra, J., & Kasting, J. F. 2016, E&PSL, 455, 7
Berner, R. A. 1992, GeCoA, 56, 3225
Berner, R. A. 1994, AmJS, 294, 56
Berner, R. A., & Berner, R. A. 2004, The Phanerozoic Carbon Cycle: CO2 and O2 (Oxford: Oxford Univ. Press on Demand)
Berner, R. A., & Kothavala, Z. 2001, AmJS, 301, 182
Berner, R. A., & Raiswell, R. 1983, GeCoA, 47, 855
Catling, D. C., Kadoya, S., Krissansen-Totton, J., & Lin, P.-C. 2019, AGUFM, 2019, PP53B
Chambers, J. 2020, ApJ, 896, 96
Checlair, J., Menou, K., & Abbot, D. S. 2017, ApJ, 845, 132
Coogan, L. A., & Dosso, S. E. 2015, E&PSL, 415, 38
Coogan, L. A., & Gillis, K. M. 2013, GGG, 14, 1771
Donnadieu, Y., Goddéris, Y., Ramstein, G., Nédélec, A., & Meert, J. 2004, Natur, 428, 303
Dorn, C., Noack, L., & Rozel, A. 2018, A&A, 614, A18
Flament, N., Coltice, N., & Rey, P. F. 2008, E&PSL, 275, 326
Foley, B. J. 2015, ApJ, 812, 36
Foley, B. J., & Smye, A. J. 2018, AsBio, 18, 873
Graham, R., & Pierrehumbert, R. 2020, ApJ, 896, 115
Haqq-Misra, J., Kopparapu, R. K., Batalha, N. E., Harman, C. E., & Kasting, J. F. 2016, ApJ, 827, 120
Höning, D., Tosi, N., & Spohn, T. 2019, A&A, 627, A48
Hu, Y., & Yang, J. 2014, PNAS, 111, 629

Ingersoll, A. P. 1969, JAtS, 26, 1191
Johnson, B. W., & Wing, B. A. 2020, NatGe, 13, 243
Kadoya, S., & Tajika, E. 2014, ApJ, 790, 107
Kadoya, S., & Tajika, E. 2019, ApJ, 875, 7
Kasting, J. F., & Ackerman, T. P. 1986, Sci, 234, 1383
Kasting, J. F., Whitmire, D. P., & Reynolds, R. T. 1993, Icar, 101, 108
Kite, E. S., & Ford, E. B. 2018, ApJ, 864, 75
Kopparapu, R. K., Ramirez, R., Kasting, J. F., et al. 2013, ApJ, 765, 131
Krissansen-Totton, J., Arney, G. N., & Catling, D. C. 2018, PNAS, 115, 4105
Krissansen-Totton, J., & Catling, D. C. 2017, NatCo, 8, 1
Kump, L. R., & Arthur, M. A. 1997, Tectonic Uplift and Climate Change (Berlin: Springer)
Maher, K., & Chamberlain, C. 2014, Sci, 343, 1502
Menou, K. 2015, E&PSL, 429, 20
Palumbo, A. M., Head, J. W., & Wordsworth, R. D. 2018, Icar, 300, 261
Paradise, A., Menou, K., Valencia, D., & Lee, C. 2019, JGRE, 124, 2087
Parrish, J. T. 1993, JG, 101, 215
Pierrehumbert, R. T. 2010, Principles of Planetary Climate (Cambridge: Cambridge Univ. Press)
Pilson, M. 1998, An Introduction to the Chemistry of the Sea (Cambridge: Cambridge Univ. Press)
Ramirez, R. M., & Kaltenegger, L. 2014, ApJL, 797, L25
Shields, A. L., Ballard, S., & Johnson, J. A. 2016, PhR, 663, 1
Sleep, N. H., & Zahnle, K. 2001, JGR, 106, 1373
Tosi, N., Godolt, M., Stracke, B., et al. 2017, A&A, 605, A71
Walker, J. C., Hays, P., & Kasting, J. F. 1981, JGR, 86, 9776
West, A. J. 2012, Geo, 40, 811
West, A. J., Galy, A., & Bickle, M. 2005, E&PSL, 235, 211